CRISPR-addressable yeast strains with applications in human G protein–coupled receptor profiling and synthetic biology

Received for publication, February 17, 2020, and in revised form, April 30, 2020 Published, Papers in Press, May 1, 2020, DOI 10.1074/jbc.RA120.013066

Jacob B. Rowe[1], **Geoffrey J. Taghon**[1], **Nicholas J. Kapolka**[1], **William M. Morgan**[1], **and Daniel G. Isom**[1,2,3,*]

From the [1]*Department of Molecular and Cellular Pharmacology, University of Miami Miller School of Medicine, Miami, Florida, USA, the* [2]*University of Miami Sylvester Comprehensive Cancer Center, Miami, Florida, USA, and the* [3]*University of Miami Center for Computational Sciences, Miami, Florida, USA*

Edited by Henrik G. Dohlman

Genome stability is essential for engineering cell-based devices and reporter systems. With the advent of CRISPR technology, it is now possible to build such systems by installing the necessary genetic parts directly into an organism's genome. Here, we used this approach to build a set of 10 versatile yeast-based reporter strains for studying human G protein–coupled receptors (GPCRs), the largest class of membrane receptors in humans. These reporter strains contain the necessary genetically encoded parts for studying human GPCR signaling in yeast, as well as four CRISPR-addressable expression cassettes, *i.e.* landing pads, installed at known safe-harbor sites in the yeast genome. We showcase the utility of these strains in two applications. First, we demonstrate that increasing GPCR expression by incrementally increasing GPCR gene copy number potentiates Gα coupling of the pharmacologically dark receptor GPR68. Second, we used two CRISPR-addressable landing pads for autocrine activation of a GPCR (the somatostatin receptor SSTR5) with its peptide agonist SRIF-14. The utility of these reporter strains can be extended far beyond these select examples to include applications such as nanobody development, mutational analysis, drug discovery, and studies of GPCR chaperoning. Additionally, we present a BY4741 yeast strain created for broad applications in the yeast and synthetic biology communities that contains only the four CRISPR-addressable landing pads. The general utility of these yeast strains provides an inexpensive, scalable, and easy means of installing and expressing genes directly from the yeast genome to build genome-barcoded sensors, reporter systems, and cell-based factories.

The yeast *Saccharomyces cerevisiae* is an important model for biotechnology and biomedical research. Because of ease of handling, rapid and robust growth, genetic encodability, haploid stability, and low cost, yeast models can be engineered to perform at scale in both laboratory and industrial settings. For example, biopharmaceuticals like insulin and hepatitis vaccines (1), organic compounds such as precursors to bioplastics (2), and biofuels (3) are produced by pathway engineering in yeast. Additionally, large-scale discovery technologies, such as yeast two-hybrid screening and display facilitate the identification of novel protein–protein interactions (4), development of antibodies (5), and selection of proteins with favorable properties such as increased thermostability and soluble secretion efficiency (6).

The *S. cerevisiae* yeast model is also important for studying human GPCR signaling. Haploid yeast of mating type *MAT**a*** have one canonical GPCR pathway, known as the pheromone pathway, that is controlled by one GPCR, Ste2 (see Fig. 1*A*) (7, 8). As shown in Fig. 1*B*, humanizing this pathway requires two primary modifications. First, the native yeast GPCR Ste2 is replaced with a human GPCR. Second, the native yeast Gα subunit Gpa1 is converted to a C-terminal chimera in which its last five residues are replaced with the last five residues of a human Gα. Together, these changes couple human GPCR activation with pheromone signaling and enable human GPCR studies in a model with greatly reduced pathway complexity and limited signaling cross-talk (9, 10). Extending the functionality of the yeast model with secondary modifications, such as installing a pheromone-responsive transcriptional reporter, can provide a readout of GPCR signaling compatible with a variety of experimental formats.

A major reason yeast models are used in a variety of applications is their genetic malleability. Relative to most cell models, yeast has long served as an attractive system for deleting, installing, and modifying genes, pathways, and genetic circuits. With the advent of CRISPR genome editing, making such modifications has become even easier (11–14). As such, the potential for high-throughput CRISPR engineering in yeast is now being realized. For example, we recently developed a high-throughput CRISPR genome editing pipeline to build several hundred humanized yeast strains for GPCR studies (15). A novel feature of these GPCR reporter strains is that human GPCRs are installed into a CRISPR-addressable landing pad at a safe harbor site known as the X-2 genome locus (14). As a result, each GPCR reporter strain we create is barcoded with a genome-integrated receptor, making it possible to identify individual GPCRs in pooled GPCR profiling experiments (15).

Here we introduce the next generation of our GPCR reporter strains that contain four CRISPR-addressable landing pads at safe harbor genome loci X-2, X-3, XI-2, and XII-5 (14). This added functionality provides an open and versatile toolbox for designing GPCR-related experiments in the yeast model. To demonstrate the utility of this resource, we used multiple landing pads to show potentiation of Gα coupling by GPCR gene copy number and autocrine GPCR activation by a genetically encoded peptide agonist. Additionally, we introduce and validate an enhanced version of the BY4741 yeast strain that contains all four CRISPR-address-

This article contains supporting information.

* For correspondence: Daniel G. Isom, disom@miami.edu.

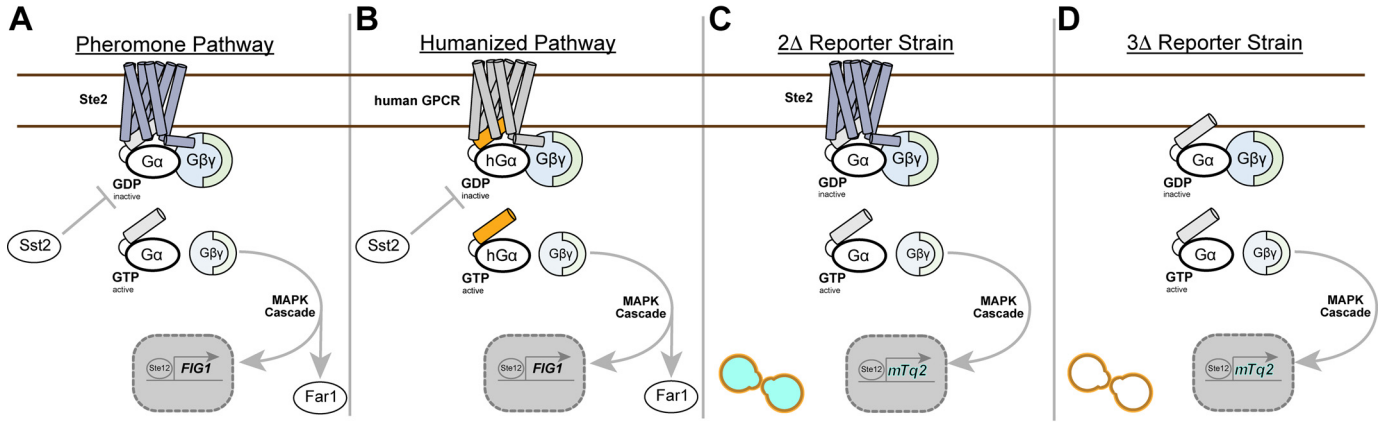

Figure 1. Humanizing the yeast pheromone pathway for GPCR studies. *A* and *B*, simplified schematics of the native (*A*) and humanized (*B*) pheromone pathway. In response to pheromone, the yeast GPCR Ste2 activates the intracellular Gα subunit to stimulate a Gβγ-driven MAP-kinase cascade that drives the expression of pheromone-responsive genes such as *FIG1*. In the humanized model, Ste2 is replaced with a human GPCR that is coupled to the pheromone pathway via a Gα subunit chimera in which the last five residues of the native yeast Gα are replaced with the last five residues of a human Gα (indicated in *orange*). *C*, in the 2Δ reporter strain, the GTPase-activating protein *SST2* is deleted, the cell cycle arrest factor *FAR1* is deleted, and *FIG1* is replaced with the transcriptional reporter mTq2. *D*, the 3Δ reporter strain is derived from the 2Δ reporter strain and has the additional deletion of the native yeast GPCR *STE2*.

able landing pads. We believe this collection of GPCR reporter and BY4741 general purpose strains will find many innovative and practical uses in the community.

Results

Ste2 expression from CRISPR-addressable landing pads rescues pheromone signaling

Engineering multipadded GPCR reporter strains required several base strains previously made in our laboratory (15). As shown in Fig. 1*C*, we deleted the GTPase-activating protein Sst2 and cell cycle arrest factor Far1 to create the 2Δ reporter strain. These gene deletions served to sensitize the pheromone pathway (*sst2*Δ) and prevent cell cycle arrest in response to pathway activation (*far1*Δ). Additionally, we installed the cyan fluorescent protein mTurquoise2 (mTq2) (16) in place of the dispensable pheromone-responsive gene *FIG1*. In our design process, this 2Δ reporter strain served as a reference control for pheromone-induced mTq2 fluorescence because it retains the yeast GPCR Ste2 in its endogenous locus.

Using the 2Δ reporter strain as a starting point, we built a series of strains to individually test the functionality of each CRISPR-addressable landing pad. We first deleted the native yeast GPCR (*ste2*Δ) to create the 3Δ reporter strain (Fig. 1*D*). As shown in Fig. 2*A*, we next created four new single-padded strains with CRISPR-addressable landing pads installed at the safe harbor chromosome loci X-2, X-3, XI-2, and XII-5. Each landing pad contained a 20-bp unique targeting sequence (UnTS) and a protospacer adjacent motif flanked by a *TEF1* promoter and a *CYC1b* terminator. To avoid off-target editing, each UnTS was computationally designed to be an artificial 20-bp DNA sequence that did not occur in the yeast genome (15).

We next conducted a series of Ste2 rescue experiments to demonstrate the functionality of each landing pad. We did this by installing the yeast GPCR Ste2 into the CRISPR-addressable landing pad of each single-padded 3Δ reporter strain (Fig. 2*B*). To test each Ste2 pad installation, we performed pheromone titrations and observed nearly identical pheromone EC_{50} values and efficacies for each pad (Fig. 2*B*). Furthermore, the pheromone EC_{50} values for the Ste2 rescues were in excellent agreement with the EC_{50} values for Ste2 expressed from its endogenous genome locus in the 2Δ reporter strain. Taken together, these data confirmed the nearly equivalent functionality of the four X-2, X-3, XI-2, and XII-5 landing pads.

Engineering four-padded GPCR reporter strains

Having validated the performance of each landing pad individually, we set out to combine all four landing pads into a panel of GPCR reporter strains that cover all possible human Gα-coupling combinations. As illustrated in Fig. 3*A*, our strain-building process began with a panel of 10 humanized GPCR reporter strains that contained a single CRISPR-addressable landing pad in the X-2 genome locus (15). In a parallel series of 30 CRISPR genome edits, we installed three additional landing pads X-3, XI-2, and XII-5 into each of the GPCR reporter strains. This process generated 20 intermediate two-padded and three-padded strains and a final set of 10 new four-padded GPCR reporter strains.

Testing the four-padded GPCR reporter strains

We next used the cyan fluorescent protein mTq2 to evaluate the individual performance of the landing pads in one of the four-padded GPCR reporter strains. To do this we installed mTq2 into the four-padded GPCR–$G\alpha_i$ reporter strain, creating four new strains, each with one copy of mTq2 in the X-2, X-3, XI-2, or XII-5 pad. As shown in Fig. 3*B*, mTq2 expressed from the X-2 and XII-5 pads gave higher fluorescence values than from the X-3 and XI-2 pads (<2-fold difference). This observation led us to conclude that mTq2 was expressed at slightly higher levels from the X-2 and XII-5 pads. We speculate that these differences in expression level result from variations in the epigenetic landscape of the different landing pad loci.

Having characterized the individual landing pads in the GPCR–$G\alpha_i$ reporter strain, we next tested all 10 four-padded GPCR reporter strains using the proton-sensing receptor GPR68. To do this, we installed GPR68 in each four-padded GPCR reporter strain, generating 40 new strains, each with one

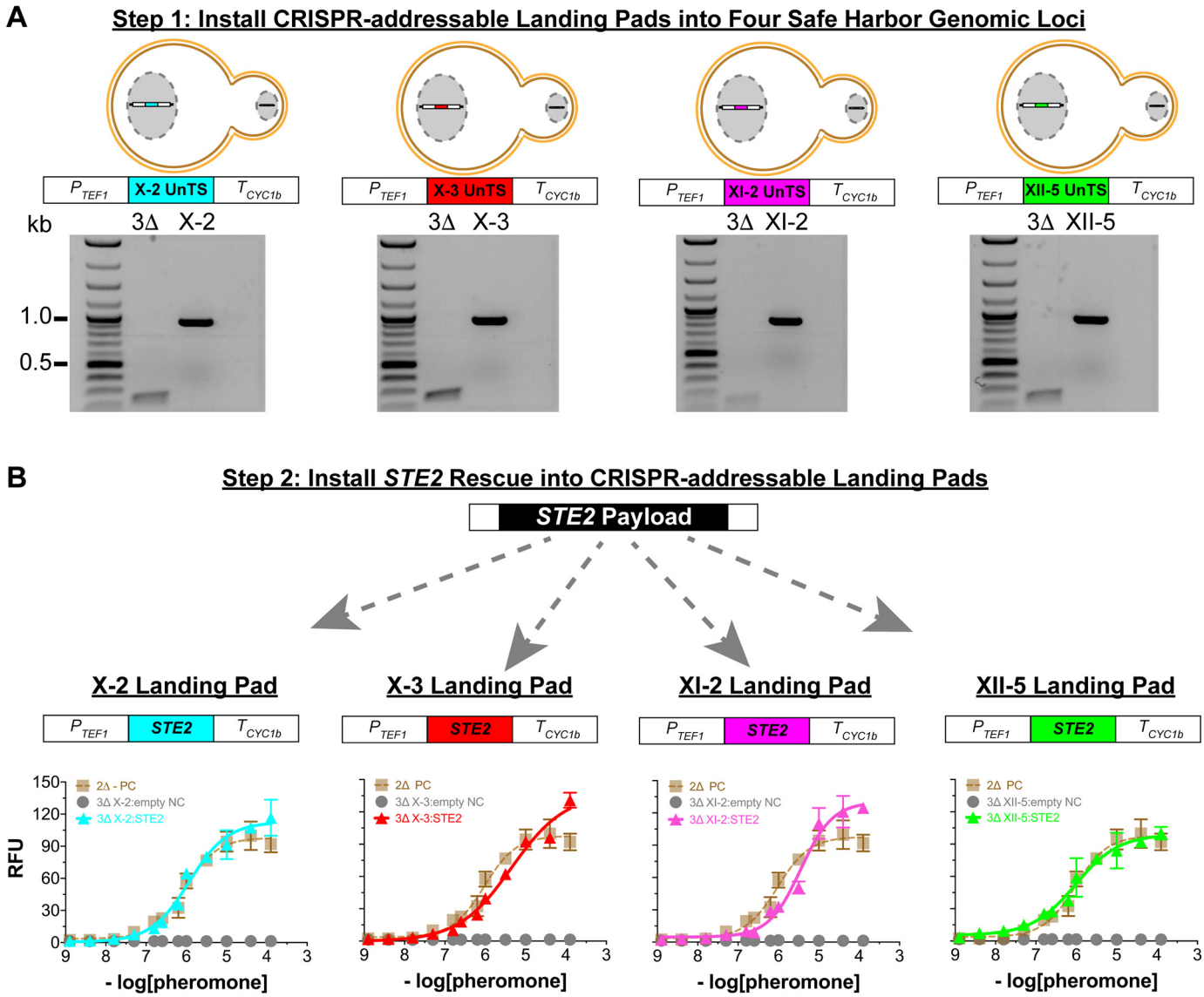

Figure 2. Installation and validation of individual CRISPR-addressable landing pads. *A*, *top panel*, The variants of our 3Δ reporter strain, each containing a single landing pad placed at known safe harbor chromosome loci X-2, X-3, XI-2, or XII-5. Each landing pad contains a 20-bp UnTS not found in the native yeast genome that provides a synthetic locus for CRISPR-addressable editing. *A*, *bottom panel*, PCR validation of landing pad installation. PCR primers used were homologous to the native genomic loci sequences flanking the landing pads. The expected product sizes were 915 bp for X-2, X-3, and XII-5 landing pads and 816 bp for the XI-2 landing pad. *B*, rescuing pheromone signaling by expressing Ste2 from each landing pad in the single-padded 3Δ reporter strains. The data are reported as relative fluorescence units (RFU) at an $A_{600\ nm}$ of 1.0 and instrument gain of 1200. Each strain was titrated with α-factor, the endogenous peptide pheromone for Ste2. *Triangles* correspond to strains expressing Ste2 from a landing pad: X-2 (*turquoise*), X-3 (*red*), XI-2 (*purple*), and XII-5 (*green*). Positive control titrations (labeled *PC*) correspond to the 2Δ reporter strain with Ste2 expressed from its native genome locus. Negative control titrations (labeled *NC*) correspond to the empty-padded 3Δ reporter strains described for *A*. *Error bars* represent the S.D. of four biological replicates.

copy of GPR68 in the X-2, X-3, XI-2, or XII-5 pad. Agonist treatment was not needed in our testing procedure because GPR68 is constitutively active below pH 7. As shown in Fig. 3*C*, we observed the same GPR68 signaling pattern for all four pads. Furthermore, pad-dependent differences in GPR68 signaling were the same as for mTq2 pad testing (Fig. 3*B*), indicating that GPR68 was also expressed at slightly higher levels from the X-2 and XII-5 pads.

Potentiating Gα coupling by incrementally increasing GPR68 gene copy number

As shown in Fig. 3*C*, GPR68 signaling was strongest in the four-padded GPCR–$G\alpha_z$ reporter strain. However, GPR68 has also been reported to signal through other Gα subunits, such as $G\alpha_q$ (17). A likely explanation for our observed GPR68–Gα coupling pattern is that GPR68–Gα interactions depend on receptor expression levels. To demonstrate the utility of the four-padded GPCR reporter strains in an application, we designed an experiment to test this possibility.

As shown in Fig. 4*A*, we installed one, two, three, and four copies of the GPR68 gene into the X-2, XII-5, X-3, and XI-2 landing pads, generating 30 additional new strains. We found that incrementally increasing GPR68 copy number led to increased signaling through the six chimeric Gα subunits $G\alpha_i$, $G\alpha_o$, $G\alpha_t$, $G\alpha_z$, $G\alpha_q$, and $G\alpha_{13}$. For example, we observed a 2.4-fold change in signaling between GPCR–$G\alpha_z$ reporter

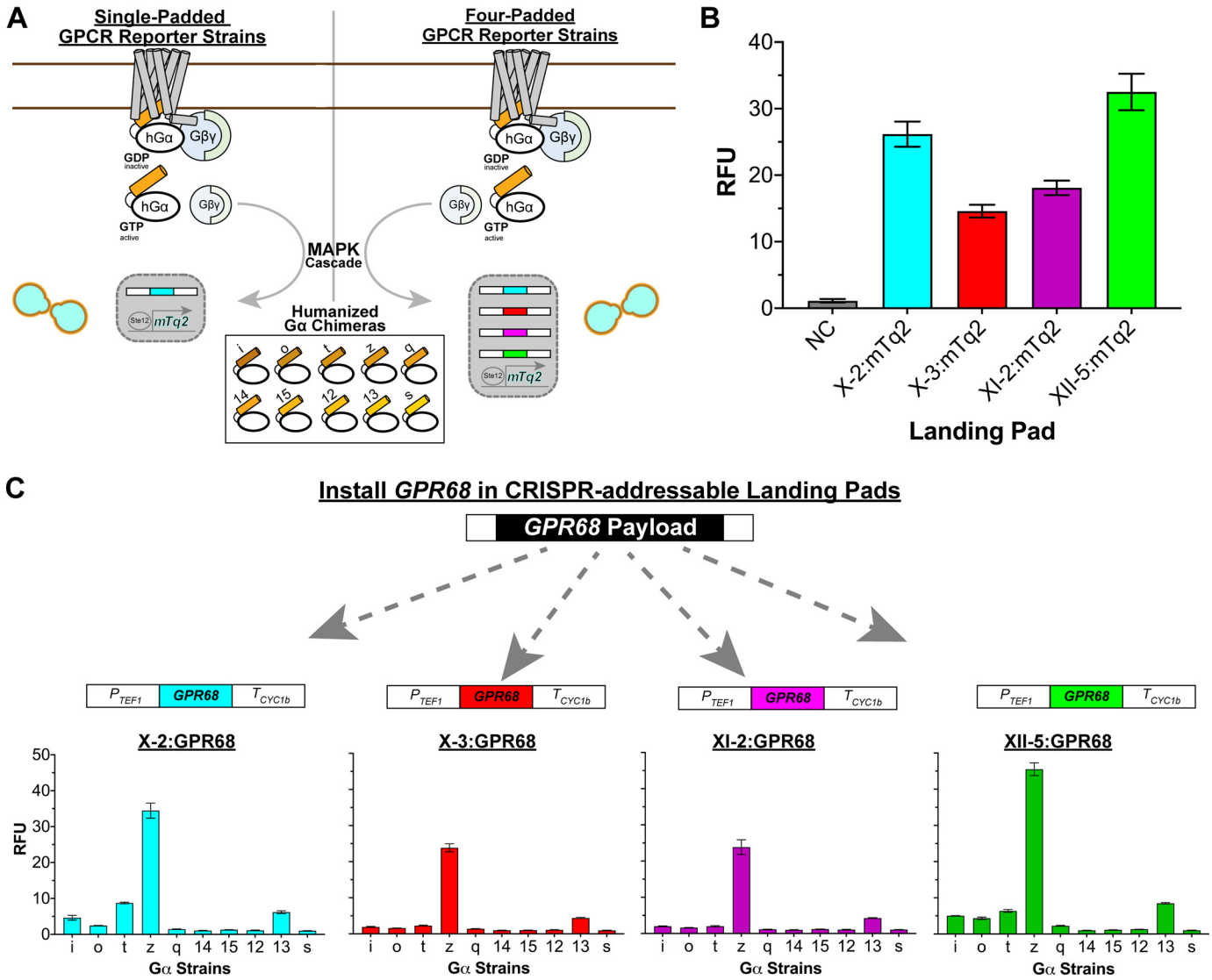

Figure 3. Engineering four-padded strains for studying human GPCRs. *A*, the engineered components of the 10 single-padded (*left panel*) and 10 four-padded (*right panel*) GPCR reporter strains used in this work. Although the full set of 10 humanized Gα chimeras are shown, each of the 10 single-padded and 10 four-padded padded GPCR reporter strains contained only one Gα chimera. *B*, validation of the functionality of each landing pad in the four-padded GPCR–$G\alpha_i$ reporter strain using mTq2. The negative control (*NC*) corresponds to the empty four-padded GPCR–$G\alpha_i$ reporter strain. *C*, validation of the functionality of each landing pad in the GPCR reporter strains using constitutively active human GPR68. The experiments were performed at pH 6.0 to activate GPR68. For *B* and *C*, the data are reported as RFU at an $A_{600\ nm}$ of 1.0 and instrument gain of 1200 for the expression of mTq2 (*B*) and GPR68 (*C*) from the X-2 (*turquoise*), X-3 (*red*), XI-2 (*purple*), or XII-5 (*green*) landing pad. *Error bars* in *B* and *C* represent the S.D. of four biological replicates.

strains with one and four pads (Fig. 4*B*). This result was typical of the other GPCR coupling combinations that signaled. Additionally, we observed the emergence of new GPCR coupling combinations with increasing GPR68 copy number. For example, two copies of GPR68, in the X-2 and XII-5 pads, were sufficient to reproduce previously observed $G\alpha_q$ coupling (Fig. 4*B*). Sequential addition of a third and fourth GPR68 copy in the X-3 and XI-2 pads increased $G\alpha_q$ signaling even further, resulting in an overall 5.2-fold change in efficacy. Together, these data demonstrate the use of GPCR gene copy number to rationally potentiate Gα coupling and signaling strength.

Autocrine activation of SSTR5 with its peptide agonist SRIF-14

In a second application of our padded GPCR reporter strains, we co-expressed the somatostatin receptor SSTR5 and its peptide agonist SRIF-14 from the X-2 (SSTR5) and XII-5 (SRIF-14) pads, generating 10 new strains. For this experiment, we used a version of the SRIF-14 peptide that included a N-terminal pre–α-factor secretion signal and a C-terminal $Flo1_{(1496-1537)}$ sequence. As illustrated in Fig. 5*A*, this added functionality directs SRIF-14 to be secreted (pre–α-factor secretion signal) and trapped (Flo1) inside the yeast cell wall where it can readily agonize SSTR5 (18).

As shown in Fig. 5*A*, expression of the trapped SRIF-14 peptide agonist from the XII-5 pad was sufficient to elicit autocrine SSTR5 signaling in the $G\alpha_i$, $G\alpha_t$, $G\alpha_z$, and $G\alpha_{15}$ reporter strains. Based on the reported nanomolar EC_{50} of SRIF-14 for SSTR5 (19), we speculated that the SRIF-14 peptide was expressed at nanomolar levels from the XII-5 pad. To confirm this, we created 20 additional GPCR reporter strains: 10 with only SSTR5 in the X-2 pad and 10 with only SRIF-14 in the XII-5 pad. Treatment of these 20 control strains with exoge-

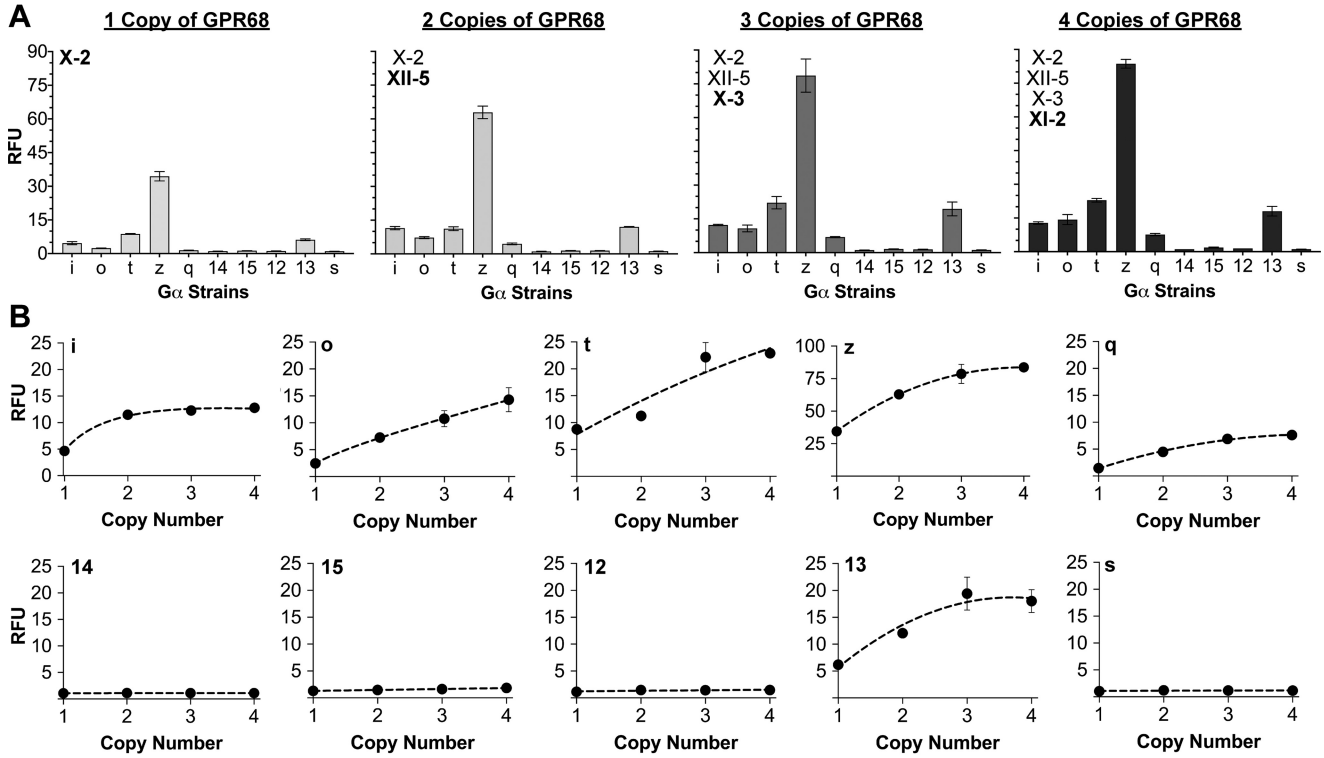

Figure 4. Increasing GPR68 copy number potentiates Gα coupling and signaling strength. *A*, Gα coupling as a function of GPR68 copy number in the 10 four-padded GPCR reporter strains. Experiments were performed at pH 6.0 to activate GPR68. The data are reported as RFU at an $A_{600\ nm}$ of 1.0 and instrument gain of 1200 for strains expressing one (X-2), two (X-2, XII-5), three (X-2, XII-5, X-3), and four (X-2, XII-5, X-3, XI-2) copies of GPR68. *B*, Gα coupling as a function of GPR68 copy number in each of the 10 four-padded GPCR reporter strains shown in *A*. The *error bars* in *A* and *B* represent the S.D. of four biological replicates.

nously added SRIF-14 peptide agonist at a concentration of 15 nM resulted in similar SSTR5 signaling levels and the same Gα-coupling pattern (Fig. 5*B*), confirming our hypothesis.

Engineering and validating a four-padded general-utility BY4741 yeast strain

Given the demonstrated utility of the four landing pads in our GPCR reporter strains, we were motivated to engineer a more general-purpose strain in the BY4741 background. To do this, we sequentially installed each landing pad into our base BY4741 strain, creating a new four-padded yeast model (Fig. 6*A*). As with our GPCR reporter strains, we used mTq2 to confirm the functionality of each pad. In all cases, mTq2 fluorescence was brighter in the BY4741 background than the GPCR–$G\alpha_i$ reporter strain background (Fig. 6*B*). This indicated that the genetic manipulations used to engineer the GPCR reporter strains (*far1*Δ, *sst2*Δ, *ste2*Δ) cause a phenotype with reduced mTq2 transcription and/or translation through the constitutive *TEF1* promoter. With the exception of the XI-2 pad, the pattern of mTq2 fluorescence intensity was the same in both the BY4741 and GPCR–$G\alpha_i$ reporter strains (Fig. 6*B*). Notably, both sets of mTq2 pad-testing strains demonstrated that mTq2 expression was lowest from the X-3 pad.

Having confirmed the functionality of the four-padded BY4741 strain, we next demonstrated its utility using four different fluorescent proteins. To do this we installed mTq2 (16), mRuby3 (20), pHluorin (21), and mNeonGreen (22) in the X-2, X-3, XI-2, and XII-5 pads, respectively. This process generated four new strains, each with a single fluorescent protein in one of the four pads. As shown in the confocal microscopy images in Fig. 6*C*, each fluorescent protein was expressed as robustly as mTq2. This was true even in the case of mRuby3, which was produced from the lower expressing X-3 landing pad. Taken together, these results demonstrated the facile engineerability and reliability of the four-padded BY4741 strain.

Discussion

Applications of the four-padded GPCR reporter strains

In this work we presented two applications of GPCR reporter strains engineered to have four CRISPR-addressable landing pads. In the first application, we used these pads to show that increasing GPR68 copy number potentiates Gα coupling and signaling strength. In the yeast model, the apparent strength of GPCR signaling is determined primarily by GPCR and G protein expression levels and a receptor's affinity for each humanized Gα subunit. Previously, we showed that G protein expression does not vary significantly between the 10 GPCR reporter strains (15). Based on these findings, the most likely explanation for our observation is that increasing the GPR68 copy number titrates the available Gα pool in each GPCR reporter strain. This conclusion is further supported by our observation that GPR68 signaling plateaued with the increasing GPR68 copy number.

In our second application, we used two of the four landing pads to co-express a GPCR (SSTR5) and a trapped version of its peptide agonist (SRIF-14). Using this approach, we were able to achieve autocrine activation of SSTR5 in several SSTR5-Gα

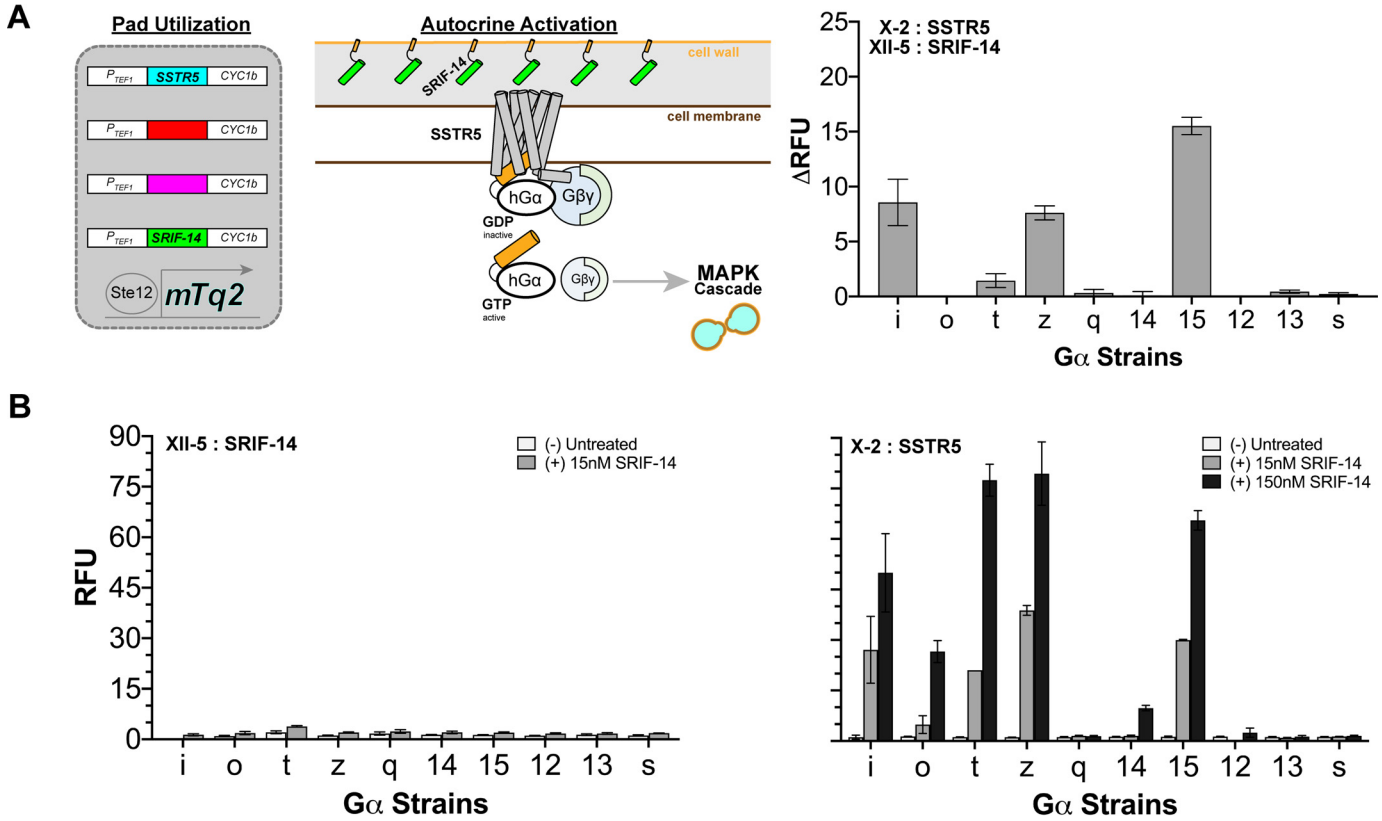

Figure 5. Autocrine activation of SSTR5 with its peptide agonist SRIF-14. *A*, *left panel*, schematic representation using two of the four landing pads for the autocrine activation of the somatostatin receptor SSTR5 (installed in the X-2 pad) with its genetically encoded peptide agonist SRIF-14 (installed in XII-5 pad). *Right panel*, autocrine activation of SSTR5 using the *panel of* 10 GPCR reporter strains illustrated in *left panel*. The data are reported as ΔRFU (*i.e.* RFU of each SSTR5/SRIF-14 autocrine strain subtracted from its counterpart untreated SSTR5-only strain) corresponding to an $A_{600\,nm}$ of 1.0 and instrument gain of 1200. *Error bars* represent the S.D. of four biological replicates. *B*, 20 control strains expressing either SRIF-14 (*left panel*) or SSTR5 (*right panel*) exogenously treated with 15 or 150 nM SRIF-14. Untreated conditions show basal activity of each strain. The data are reported as RFU corresponding to an $A_{600\,nm}$ of 1.0 and instrument gain of 1200. *Error bars* represent the S.D. of three (SSTR5; *right panel*) or four (SRIF-14; *left panel*) biological replicates.

reporter strains. In principle, this application could be extended to any GPCR–peptide agonist pair or any interaction between a GPCR and a genetically encodable ligand, including proteins such as chemokines and nanobodies. Perhaps the greatest benefit of pad-based autocrine secretion is that it circumvents the time and expense of producing and purifying genetically encodable GPCR ligands in the lab or purchasing them from commercial sources.

There are myriad applications of the GPCR reporter strains beyond those presented here. Our laboratory is using these strains to study receptor mutations on an unprecedented scale, identify and characterize new pH-sensing GPCRs, discover new GPCR ligands and drugs, explore GPCR chimera space, and dissect the details of biased GPCR signaling. By sharing these strains with the community, we anticipate that the number and diversity of strain applications will continue to grow and that the insights they provide will complement and enhance our understanding of GPCR studies done in their more native systems.

The utility of the enhanced BY4741 strain

There are also few limitations on developing novel applications using the four-padded BY4741 strain. Installation of genetically encoded biosensors, modified yeast proteins (*e.g.* tagged or mutated versions of native yeast proteins), and rescue components, such as the Ste2 rescue experiments in this work, are but a few examples of practical uses. This utility could be extended even further to include the heterologous expression of protein components for building small enzymatic and metabolic pathways. Larger pathways could be accommodated by installing additional pads using the methods described in this work. In principle, this approach is limited only by the compatibility of heterologous proteins with the yeast model.

Building and standardizing padded yeast strains into the future

We created the CRISPR-addressable strains described in this work to suit both the specific needs of our laboratory and the general needs of the wider research community. Analogous to software, we view these strains as contributing to an open-source effort. As discussed, there are many more opportunities to install and test landing pads in safe harbor sites. What is more, the design of these pads is left to the discretion of the end user and can be adapted to suit specific requirements. For example, all four of the landing pads described in this work had a constitutive *TEF1* promoter and *CYC1b* terminator. However, various promoters, whether constitutive or inducible, could be combined with various terminators to build a wide array of synthetic and hypothesis-testing strains. Such efforts

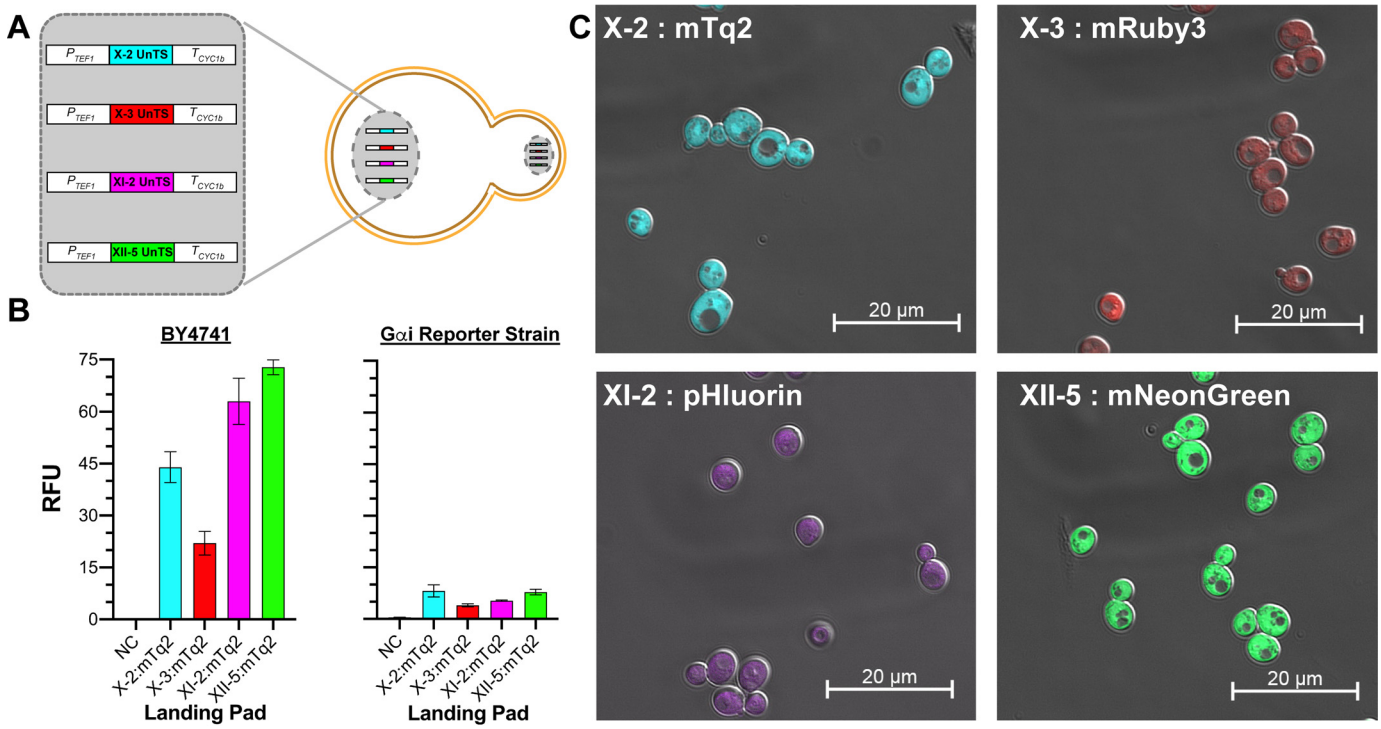

Figure 6. Installation and testing of genome-integrated landing pads in the BY4741 strain. *A*, the four genome-integrated landing pads of the enhanced BY4741 strain. *B*, *left panel*, validation of the functionality of each landing pad in the four-padded BY4741 strain using mTq2. *Right panel*, mTq2 expression from each of the landing pads in the four-padded GPCR–Gα_i reporter strain. The data in both panels are reported as RFU at an $A_{600\ nm}$ of 1.0 and instrument gain 1000. The negative controls (*NC*) correspond to the empty four-padded BY4741 strain or GPCR–Gα_i reporter strain, respectively. *Error bars* represent the S.D. of four biological replicates. *C*, validation of each landing pad using confocal microscopy to quantify the fluorescence of mTq2, mRuby3, pHluorin, and mNeonGreen expressed from the X-2, X-3, XI-2, and XII-5 pads, respectively.

could begin with a base strain, such as BY4741, or build upon the four-padded strains described here.

In classical yeast genetics, exogenous DNA payloads are most often installed at genome loci such as *HO* (23) or at intergenic loci anecdotally identified by individual labs as having no apparent phenotypic consequences. Thus, there is no clear consensus on where to install heterologous proteins or genetic tools within the yeast genome. The safe harbor sites identified by Ronda *et al.* (14) afford us the opportunity to begin building this consensus. We chose the X-2, XII-5, X-3, and XI-2 safe harbor loci because they were among the best performing sites in initial studies (14). However, with more than 10 safe harbor sites known (14) and with efforts to identify many more (24), the community is developing an extraordinary latitude for expanding CRISPR-addressable functionality in yeast strains used for biomedical research, synthetic biology, and industrial applications. With these advances comes the opportunity to standardize pad-based strain-building initiatives. Such an effort could lead to unprecedented growth in the availability of robust, reliable, and shareable synthetic yeast strains.

Experimental procedures

Materials

Yeast extract, yeast nitrogen base, peptone, tryptone, and 5-fluoroorotic acid (5FOA) were purchased from Research Products International (Mt. Prospect, IL, USA). Low-fluorescence yeast nitrogen base used for preparing screening medium was purchased from Formedium (Hunstanton, UK). Complete supplement mixture and complete supplement single dropout (without uracil) mixture were purchased from MP Biomedicals (Solon, OH, USA). Screening medium was adjusted to desired pH with HCl or KOH and were buffered with potassium phosphate dibasic (Alfa Aesar, Ward Hill, MA, USA) and MES hydrate (Research Products International). SRIF-14 peptide for exogenous applications (Fig. 5*B*) was purchased from Cayman Chemical Company (Ann Arbor, MI, USA; catalog no. 54472-66-1).

Oligonucleotides and gBlocks

The complete list of primers and gBlocks (IDT, Coralville, IA) used in this study can be found in supporting data set 1.

Plasmids

All CRISPR plasmids used in this work were derived from pML104. Four new versions of the pML104 plasmid were made to first install each landing pad into the genome loci X-2, X-3, XI-2, and XII-5. Four additional versions of the pML104 plasmid were then made for targeting DNA payloads to the artificial guide sequences within each CRISPR-addressable landing pad. The name and sequence of each new pML104 plasmid construct and its specific guide sequence are listed in supporting data set 2, along with any other plasmids used in this study. All plasmids were maintained in the *Escherichia coli* strain DH5α (New England BioLabs, Ipswich, MA, USA) and purified using the EZ plasmid miniprep kit (EZ BioResearch, St. Louis, MO, USA). Genes for GPR68 and SSTR5 were sourced from the PRESTO-TANGO plasmid library (25).

Strains

The complete list of 150 strains made over the course of this study can be found in supporting data set 3.

Media, Buffers, and Solutions

The complete list of growth media, buffers, and solutions used in this study can be found in supporting data set 4. Growth media, buffers, and solutions prepared at specified pH values were measured using an Accumet XL150 pH meter (Fisher Scientific, Hampton, NH, USA).

CRISPR protocol

Preparing base strains—Base yeast strains were struck from glycerol onto YPD plates and incubated at 30 °C for 1–2 days. Colonies were picked into 5 ml of YPD and grown at 30 °C shaking (200 rpm) until an A_{600} of 0.2–1.0 was reached.

Preparing cells for transformation—Log-phase cultures were centrifuged (3000 × *g* for 3 min), harvested, and washed with 5 ml of TE. The cells were centrifuged, harvested, washed with 5 ml of LiOAc mix, centrifuged again, and resuspended in 200 μl of LiOAc mix.

Preparing transformation mixtures—The solution for a single yeast transformation reaction comprised 175 μl of PEG mix, 250 ng of CRISPR plasmid, 20 μl of DNA payload (5–15 μg of DNA total), and 5 μl of salmon sperm DNA (boiled at 100 °C for 10 min and then placed on ice immediately after boiling).

Transformation procedure—50 μl of prepared cells were added to the transformation mixture described above. The mixtures were briefly vortexed, then incubated at room temperature for 30 min, spiked with 12 μl of DMSO, vortexed, and incubated at 42 °C for 15 min. The mixtures were then centrifuged (5000 × *g* for 1 min), and the harvested cells were resuspended in 200 μl of YPD by gently pipetting 5–8 times. The resuspended cells were plated onto SCD-U agar plates and grown at 30 °C for 3 days. This protocol works for well for plating on both large (100-mm Petri dishes, 100-μl plate) and small (22-mm 12-well Petri dishes, 35-μl plate) agar plates.

Validation and storage of yeast strains

Genomic DNA extraction to confirm payload integration—Transformed colonies were picked into SCD-U liquid medium and grown at 30 °C for 1–2 days. Genomic DNA (gDNA) was then extracted and purified as previously described (15). Briefly, 100 μl of resuspended cells were added to a 1.5-ml Eppendorf tube, centrifuged (15,000 × *g* for 3 min), harvested, and resuspended in 100 μl of extraction buffer. The cells were then resuspended by vortexing and incubated at 70 °C for 10 min. 300 μl of 100% EtOH was added to the mixture, which was then vortexed and centrifuged. The gDNA pellet was washed with 70% EtOH and dried at 70 °C for 10 min. The dried gDNA pellet was resuspended in 50 μl of nuclease-free H_2O by thorough vortexing and pipetting and centrifuged (15,000 × *g* for 30 s), and 25 μl of supernatant containing the purified gDNA was transferred to a clean 1.5-ml Eppendorf tube. 1 μl of purified gDNA was then used to PCR-verify integration of the desired DNA payload. PCRs were resolved on 1% agarose gels and imaged using an Amersham Biosciences Imager 600 (GE Healthcare).

Removing the CRISPR plasmid by counter-selection—For a given CRISPR reaction, one strain containing the correctly integrated gene was struck from SCD-U liquid medium onto a CSM + 5FOA plate and placed at 30 °C until colonies were present (≈2 days).

Yeast glycerol stocks—One colony was picked from a CSM + 5FOA plate into 3 ml of YPD and grown at 30 °C overnight. Using this culture, gDNA was purified and PCR-verified as described under "Genomic DNA extraction to confirm payload integration." For a single PCR-verified strain, 15% (v/v) glycerol stocks were prepared for long-term storage at −80 °C.

Landing pad design and integration

Landing pad design—The X-2 landing pad was synthesized in a pMARQ plasmid (Invitrogen), and the X-3, XI-2, and XII-5 landing pads were synthesized as gBlocks (IDT). All four CRISPR-addressable landing pads contained a unique core sequence (a 32-bp synthetic sequence consisting of a 20-bp UnTS, 3-bp protospacer adjacent motif site, and 9 bp of buffer DNA) flanked by a P_{TEF1} promoter (419 bp) and T_{CYC1b} terminator (242 bp). Additionally, each landing pad cassette was flanked upstream and downstream by 110 bp of homology to the X-2, X-3, XI-2, or XII-5 chromosome loci.

Landing pad integration—DNA payloads were prepared by PCR amplifying the gBlocks described under "Landing pad design." Using the CRISPR protocol described above, each DNA payload and its cognate CRISPR plasmid (pML104 X-2, X-3, XI-2, or XII-5) were co-transformed into the desired base yeast strain. Integration of each landing pad was then validated as described under "Validation and storage of yeast strains" and confirmed via Sanger sequencing (Eurofins Genomics, Louisville, KY, USA). Four-padded strains were created by installing the landing pads sequentially in the following order: X-2 (first), XII-5, X-3, and XI-2 (last).

Using the CRISPR-addressable landing pads.

Preparing the DNA payload—DNA payloads originating from plasmid sources (*i.e.* mTq2, pHluorin, mRuby3, GPR68, and SSTR5) were prepared via two rounds of PCR. The first round of PCR amplified the desired gene, whereas the second round of PCR extended the amplified gene product with 60 bp of homology to the *TEF1* promoter and *CYC1b* terminator. In some case, the 60 bp of *TEF1* and *CYC1b* homology could be provided directly by PCR primers and introduced in one PCR (Ste2 sourced from the yeast genome and the mNeonGreen and SRIF-14 sourced from gBlocks).

CRISPR-addressable gene integration—DNA payloads were installed into the desired landing pads using the CRISPR protocol described above, and the cognate CRISPR plasmid (*i.e.* pML104 X-2 UnTS, X-3 UnTS, XI-2 UnTS, or XII-5 UnTS). For strains in which a fluorescent protein gene was integrated, transformant colonies on SCD-U plates were imaged using an Amersham Biosciences Imager 600 (excitation filters, 460 and 520 nm) to identify fluorescent colonies. All integrations were validated using the approach described under "Validation and storage of yeast strains."

Fluorescence measurements

A CLARIOstar multimode microplate reader (BMG LabTech, Offenburg, Germany) was used for all microplate-based fluorescence (bottom read; 10 flashes/well; excitation: 430/10 nm, dichroic filter: LP 458 nm, emission filter: 482/16 nm) and absorbance (22 flashes/well; excitation filter, 600 nm) measurements.

Sample preparation—Strains were struck from glycerol onto YPD plate(s) and grown at 30 °C for 1–2 days. Four colonies per strain were picked from YPD into 96-well deep-well blocks (Greiner Bio-One; catalog no. 780271-FD) containing 500 μl of SCD. Screening medium was adjusted to pH 6.5 and grown at 30 °C until they reached log-phase growth ($A_{600\ nm}$ = 0.2–1.5). 200-μl aliquots of cells were transferred to a 96-well plate(s), centrifuged (3000 × *g* for 5 min), harvested, and resuspended in 200 μl of screening medium adjusted to pH 6.0 (pH 7.0 for SSTR5 and SRIF-14 experiments). Resuspended cells were used to prepare 200 μl of normalized cultures in 96-well format having an $A_{600\ nm}$ of 0.05 using a Biomek NX^P liquid-handling robot. Plates with normalized cultures were covered with porous film (Diversified Biotech; catalog no. BERM-2000), shaken (1200 rpm for 30 s) on a MixMate microplate shaker (Eppendorf, Hamburg, Germany), and incubated at 30 °C for ≈18 h.

Data acquisition—All data were collected from four biological replicates (*i.e.* colonies), the fluorescence of which was measured over a linear dilution series. These data were fit in Prism to generate slope and intercept values that were used to extrapolate mTq2 fluorescence to a standardized $A_{600\ nm}$ value of 1.0. *Error bars* represent the standard error of the fitted slopes, which in Prism equates to the standard deviation. All samples were assayed as 50-μl aliquots in black 384-well clear-bottom plates (Greiner Bio-One; catalog no. 781096).

Confocal microscopy

Colonies were picked into screening medium, pH 6.0, and grown at 30 °C with shaking until an $A_{600\ nm}$ of 1.0 was reached. The cultures were then centrifuged (3000 × *g* for 3 min), harvested, and the cells were resuspended in 200 μl of fresh pH 6.0 medium. 2 μl of cells were added to a 75 × 25 × 1-mm microscope slide (VWR; catalog no. 16004-422) and covered with a 22 × 22-mm no. 1.5 glass coverslip (VWR; catalog no. 48366-227). The cells were imaged using an LSM800 confocal microscope (Carl Zeiss) at 63× magnification. For a given field, both differential interference contrast and fluorescence images were acquired, which were overlaid and further processed using Zeiss's Zen software. Fluorescence images were acquired using excitation lasers of 405 nm (mTq2; 2.00% intensity), 561 nm (mRuby3; 2.00% intensity), 405 and 488 nm (pHluorin; 3.50% and 4.50% intensity, respectively), and 488 nm (mNeonGreen; 0.04% intensity).

Data availability

All relevant data, protocols, and results of analyses are included in the main text. Yeast strains are available upon request.

Author contributions—J. B. R., N. J. K., and D. G. I. conceptualization; J. B. R. formal analysis; J. B. R. validation; J. B. R., G. J. T., N. J. K., and W. M. M. investigation; J. B. R., G. J. T., N. J. K., and D. G. I. methodology; J. B. R. and D. G. I. writing-original draft; J. B. R., G. J. T., N. J. K., and D. G. I. writing-review and editing; D. G. I. supervision; D. G. I. funding acquisition; D. G. I. project administration; W. M. M. technical support.

Funding and additional information—This work was supported by NIGMS, National Institutes of Health Grant R35GM119518 and by the Common Fund for Illuminating the Druggable Genome through National Institutes of Health Grant R03TR002908 (to D. G. I.). The content is solely the responsibility of the authors and does not necessarily represent the official views of the National Institutes of Health.

Conflict of interest—The authors declare that they have no conflicts of interest with the contents of this article.

Abbreviations—The abbreviations used are: GPCR, G protein–coupled receptor; UnTS, unique targeting sequence; gDNA, genomic DNA; 5FOA, 5-fluoroorotic acid; RFU, relative fluorescence unit(s).

References

1. Nielsen, J. (2013) Production of biopharmaceutical proteins by yeast: advances through metabolic engineering. *Bioengineered* **4,** 207–211 CrossRef Medline
2. Horwitz, A. A., Walter, J. M., Schubert, M. G., Kung, S. H., Hawkins, K., Platt, D. M., Hernday, A. D., Mahatdejkul-Meadows, T., Szeto, W., Chandran, S. S., and Newman, J. D. (2015) Efficient multiplexed integration of synergistic alleles and metabolic pathways in yeasts via CRISPR-Cas. *Cell Syst.* **1,** 88–96 CrossRef Medline
3. Tran, T. N. T., Breuer, R. J., Avanasi Narasimhan, R., Parreiras, L. S., Zhang, Y., Sato, T. K., and Durrett, T. P. (2017) Metabolic engineering of *Saccharomyces cerevisiae* to produce a reduced viscosity oil from lignocellulose. *Biotechnol. Biofuels* **10,** 69 CrossRef Medline
4. Uetz, P., Giot, L., Cagney, G., Mansfield, T. A., Judson, R. S., Knight, J. R., Lockshon, D., Narayan, V., Srinivasan, M., Pochart, P., Qureshi-Emili, A., Li, Y., Godwin, B., Conover, D., Kalbfleisch, T., *et al.* (2000) A comprehensive analysis of protein–protein interactions in *Saccharomyces cerevisiae*. *Nature* **403,** 623–627 CrossRef Medline
5. Bradbury, A. R., Sidhu, S., Dübel, S., and McCafferty, J. (2011) Beyond natural antibodies: the power of *in vitro* display technologies. *Nat. Biotechnol.* **29,** 245–254 CrossRef Medline
6. Shusta, E. V., Holler, P. D., Kieke, M. C., Kranz, D. M., and Wittrup, K. D. (2000) Directed evolution of a stable scaffold for T-cell receptor engineering. *Nat. Biotechnol.* **18,** 754–759 CrossRef Medline
7. Bardwell, L. (2005) A walk-through of the yeast mating pheromone response pathway. *Peptides* **26,** 339–350 CrossRef Medline
8. Wang, Y., and Dohlman, H. G. (2004) Pheromone signaling mechanisms in yeast: a prototypical sex machine. *Science* **306,** 1508–1509 CrossRef Medline
9. Dowell, S. J., and Brown, A. J. (2002) Yeast assays for G-protein–coupled receptors. *Receptors Channels* **8,** 343–352 Medline
10. Dowell, S. J., and Brown, A. J. (2009) Yeast assays for G protein–coupled receptors. *Methods Mol. Biol.* **552,** 213–229 CrossRef Medline
11. Besada-Lombana, P. B., McTaggart, T. L., and Da Silva, N. A. (2018) Molecular tools for pathway engineering in *Saccharomyces cerevisiae*. *Curr. Opin Biotechnol.* **53,** 39–49 CrossRef Medline
12. DiCarlo, J. E., Norville, J. E., Mali, P., Rios, X., Aach, J., and Church, G. M. (2013) Genome engineering in *Saccharomyces cerevisiae* using CRISPR-Cas systems. *Nucleic Acids Res.* **41,** 4336–4343 CrossRef Medline
13. Laughery, M. F., Hunter, T., Brown, A., Hoopes, J., Ostbye, T., Shumaker, T., and Wyrick, J. J. (2015) New vectors for simple and streamlined CRISPR-Cas9 genome editing in *Saccharomyces cerevisiae*. *Yeast* **32,** 711–720 CrossRef Medline

14. Ronda, C., Maury, J., Jakočiunas, T., Jacobsen, S. A., Germann, S. M., Harrison, S. J., Borodina, I., Keasling, J. D., Jensen, M. K., and Nielsen, A. T. (2015) CrEdit: CRISPR mediated multi-loci gene integration in *Saccharomyces cerevisiae*. *Microb Cell Fact* **14,** 97 CrossRef Medline
15. Kapolka, N., Taghon, G. J., Rowe, J. B., Morgan, W. M., Enten, J. F., and Ison, D. G. (2020) DCyFIR: a high-throughput CRISPR platform for multiplexed G protein–coupled receptor profiling and ligand discovery. *bioRxiv* CrossRef
16. Goedhart, J., von Stetten, D., Noirclerc-Savoye, M., Lelimousin, M., Joosen, L., Hink, M. A., van Weeren, L., Gadella, T. W., Jr., and Royant A. (2012) Structure-guided evolution of cyan fluorescent proteins towards a quantum yield of 93%. *Nat. Commun.* **3,** 751 CrossRef Medline
17. Huang, X. P., Karpiak, J., Kroeze, W. K., Zhu, H., Chen, X., Moy, S. S., Saddoris, K. A., Nikolova, V. D., Farrell, M. S., Wang, S., Mangano, T. J., Deshpande, D. A., Jiang, A., Penn, R. B., Jin, J., *et al.* (2015) Allosteric ligands for the pharmacologically dark receptors GPR68 and GPR65. *Nature* **527,** 477–483 CrossRef Medline
18. Ishii, J., Yoshimoto, N., Tatematsu, K., Kuroda, S., Ogino, C., Fukuda, H., and Kondo, A. (2012) Cell wall trapping of autocrine peptides for human G-protein–coupled receptors on the yeast cell surface. *PLoS One* **7,** e37136 CrossRef Medline
19. O'Carroll, A. M., Raynor, K., Lolait, S. J., and Reisine, T. (1994) Characterization of cloned human somatostatin receptor SSTR5. *Mol. Pharmacol.* **46,** 291–298 Medline
20. Bajar, B. T., Wang, E. S., Lam, A. J., Kim, B. B., Jacobs, C. L., Howe, E. S., Davidson, M. W., Lin, M. Z., and Chu, J. (2016) Improving brightness and photostability of green and red fluorescent proteins for live cell imaging and FRET reporting. *Sci. Rep.* **6,** 20889 CrossRef Medline
21. Miesenböck, G., De Angelis, D. A., and Rothman, J. E. (1998) Visualizing secretion and synaptic transmission with pH-sensitive green fluorescent proteins. *Nature* **394,** 192–195 CrossRef Medline
22. Shaner, N. C., Lambert, G. G., Chammas, A., Ni, Y., Cranfill, P. J., Baird, M. A., Sell, B. R., Allen, J. R., Day, R. N., Israelsson, M., Davidson, M. W., and Wang, J. (2013) A bright monomeric green fluorescent protein derived from Branchiostoma lanceolatum. *Nat. Methods* **10,** 407–409 CrossRef Medline
23. Voth, W. P., Richards, J. D., Shaw, J. M., and Stillman, D. J. (2001) Yeast vectors for integration at the HO locus. *Nucleic Acids Res.* **29,** E59–E59 CrossRef Medline
24. Wu, X. L., Li, B. Z., Zhang, W. Z., Song, K., Qi, H., Dai, J. B., and Yuan, Y. J. (2017) Genome-wide landscape of position effects on heterogeneous gene expression in *Saccharomyces cerevisiae*. *Biotechnol Biofuels* **10,** 189 CrossRef Medline
25. Kroeze, W. K., Sassano, M. F., Huang, X. P., Lansu, K., McCorvy, J. D., Giguère, P. M., Sciaky, N., and Roth, B. L. (2015) PRESTO-Tango as an open-source resource for interrogation of the druggable human GPCRome. *Nat. Struct. Mol. Biol.* **22,** 362–369 CrossRef Medline